SEMARAK ILMU PUBLISHING

Journal of Advanced Research in Fluid Mechanics and Thermal Sciences

Journal homepage:
https://semarakilmu.com.my/journals/index.php/fluid_mechanics_thermal_sciences/index
ISSN: 2289-7879

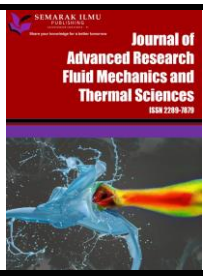

Investigation on the Performance of Micro Wind Turbine Rotor Using Whale-Inspired Blade Based on Low Wind Regime

Bashir Isyaku Kunya[1,*], Bala Abdullahi[1], Najib Aminu Ismail[2]

[1] Department of Mechanical Engineering, Kano University of Science and Technology, Wudil, Nigeria
[2] High-Speed Reacting Flow Laboratory, Faculty of Mechanical Engineering, Universiti Teknologi Malaysia (UTM), Johor, Malaysia

ARTICLE INFO

Article history:
Received 7 June 2022
Received in revised form 15 November 2022
Accepted 28 November 2022
Available online 18 December 2022

ABSTRACT

The potential of wind energy in a country varies depending on the region. For example, in Northern regions of Nigeria, cities like Minna, Sokoto, Kano and Jos are the most potential locations and experience not more than 5.24 m/s mean wind speed with Jos having the highest average wind speed. In most cases internationally wind turbines are design to operate at the rated wind speed much greater than mean wind speeds in Nigeria (in most cases above 8 m/s). Installation of these wind turbines in a similar location to Nigeria (in terms of wind speed condition) will significantly decrease their performance. Therefore, it become necessary to design and produce wind turbines that will function efficiently in low wind speed locations. One of the technologies to improve wind turbine rotor blade effectiveness in low wind regime is to boost the operating angle of the wind turbine, and hence the prospect for the improvement of wind turbine performance. An innovative way recognized previously by some researchers for increasing the working angle of the blade at low wind speed for improved performance is modification of wind turbine blade leading edge. This research studied three-bladed wind turbine rotor with modified blades leading edges (by incorporating sinusoidal bumps) at low wind speeds using CFD method. Two CAD models of wind turbine blades based on 0.8m three-bladed wind turbine rotor were modelled and simulated. One blade model is having straight leading edge (N-Blade) and the other having bumpy leading edge (M-Blade). Both models have NASA LS (1)-0413 cross-section profile. Simulations were run using ANSYS 20 from a velocity of 2 m/s to 10 m/s at the interval of 2m/s considering TSR of 6 and 8. At a TSR of 6, the coefficients of performance (Cp) values are not equal, with the straight blade having better performance than the bumpy blade at all velocities tested; the Cp values of blade with straight leading edge are 0.180, 0.267, 0.300, 0.313, 0.322 at respective velocities of 2, 4, 6, 8, and 10m/s, while Cp values of blade with bumpy leading edge at the same velocities are 0.165, 0.250, 0.281, 0.294, and 0.303 respectively. At a TSR of 8, the C_P values closely match for both straight and bumpy blade at all velocities tested for. Simulations were further run at constant angular velocity of 120 rad/s for a TSR of 2, 4, and 10, where the peak performance occurs is around TSR of 6 and 8. For instance, the Cp values of M-Blade are 0.022, 0.173, 0.294, 0.313, and 0.116 respectively at the TSR of 2, 4, 6, 8, and 10. At TSR of 2, 4, 8 and 10, the performance of both airfoils closely matches except at a TSR of 6 where the N-Blade Cp value is 0.313 and is better than that of M-Blade Cp value (0.294). It shows that the blade leading edge modification could not have advantage at all flow

* *Corresponding author.*
E-mail address: kunyabashir@yahoo.com

https://doi.org/10.37934/arfmts.101.2.184196

Journal of Advanced Research in Fluid Mechanics and Thermal Sciences
Volume 101, Issue 2 (2023) 184-196

Keywords:
Wind turbine rotor; rotor blade; low wind speed; coefficient of performance; torque; blade leading edge

conditions and size of the HAWT blades; it shows no advantage on the performance of the rotor blade tested in this research at the velocities at which the simulation was conducted.

1. Introduction

Wind power is a free and inexhaustible (renewable) source of energy which releases no pollution in to the air or water, and does not contribute to global warming. And unlike most other electricity sources, wind turbines do not consume water or fuel. Adding wind power to the energy supply diversifies the natural energy portfolio and reduces Nation's reliance on fuels thus, stabilizing the cost of electricity, reducing vulnerability to price hikes and supply disruptions, and bolstering the security of our national energy supply.

The potential of wind power in a country varies from one region to another. For instance, most potential locations in Nigeria experience not greater than 5.24 m/s mean wind speed [1]. However, Jos has the highest average wind speed; 10.12m/s according to Ahmed *et al.,* [2] and 13.8m/s according to Oyewole [3]. In most cases internationally wind turbines are design to operate at the rated wind speed much greater than mean wind speeds in Nigeria (in most cases above 8 m/s). Installation of these wind turbines in a location similar to Nigeria (in terms of wind speed condition) will decrease their performance significantly. Therefore, it become necessary to design and produces wind turbines that will function efficiently in the low wind speed locations. One of the technologies to improve wind turbine rotor blade effectiveness in low wind regime is to increase the operating angle of the wind turbine, and hence the prospect for the improvement of wind turbine performance.

Imitating the bumpy geometrical shape of pectoral flippers (fins) of Humpback whales (Megaptera Novaeangliae) (Figure 1) can improve performance of wind turbine blade the similar way it does for the humpback whale. This animal uses the geometry of their fins as advantage to delaying stall despite using increased working angle. This enables it do very tight movement in order to catch their own food [4]. Miklosovic *et al.,* [5] evaluated the effectiveness of tubercles (bumps) of a humpback whale pectoral flipper by creating two computer models representing their shapes. The result of their work represents a performance improvement that a stall was delayed for the model with bumps despite the increase of working angle, the angle of attack (AOA) (12 to 17.5 degrees).

Fig. 1. Humpback whale [6]

Hansen *et al.,* [7] is among other researchers who worked in this area. They experimentally studied the influence of bump height and sinusoidal wavelength at the leading edge (LE) of physical models made from two NASA airfoils family over a range of Reynolds number (Re) (1.2×10^5 to 2.74×10^5). On testing the models, airfoils with LE bumps have greater maximum lift coefficient and greater stall angle. And by increasing wavelength, stall characteristic improved but slightly reduced the maximum lift coefficient. The bumps benefited one model over the other because they have different cross-section shape. A numerical study at somehow lower Re (between 65,000 and 1,000,000) was conducted by Gawad [8] using NASA 0012 airfoil. The uppermost lift coefficient

increases with Reynolds number, drag has increased and stall was delayed by bumps. Based on numerical investigation done by Carija *et al.,* [9] at a Re of 1.8 x 10^6 using a turbine blade with NACA 0012 cross-section, LE bumps increased Lift coefficient from 3 to 9.5 per cent and decreased drag at an AOA larger than 10-degree, and very little changes in the lift and drag demonstrated for the AOA below 10-degree. Stall was delayed by the sinusoidal leading edge and increased the stalling AOA by around five degrees.

An airfoil (S809) with relatively thicker cross-section was numerically examined by Asli [10] at 1,000,000 Re, and it shown that at low AOA before stall, lift coefficient of airfoil with LE bumps decreased slightly than that of the model with straight LE. But flow separation caused the baseline airfoil lift coefficient decreased sharply while the modified airfoil has a gradual stall trend. Similar trend was obtained by Zhao *et al.,* [11] using numerical analysis on NACA 63_4-021 airfoil, and according to them the improved airfoil performance was as a results of reduced flow separation around both crest and trough sections of the bumpy airfoil.

One of the research works conducted on other means of airfoil modification related to aircraft is on modification of ONERA M6 wing by Munshi [12]. He used winglets to reduce tip vortices. Flow characteristics was examined at 30-, 60- and 75-degree winglets cant angle and by varying AOA (from 3 to 6 degrees). It shows that to a certain degree of AOA, the modification improved lift to drag ratio better than the usual plane wing without winglets. As AOA was increased further to larger degrees it resulted in decreasing the lift to drag ratio, hence reducing its performance.

Two-dimensional (2-D) flow study on performance of airfoil with NASA LS (1)-0413 profile by Kunya *et al.,* [13] at low Re (49000) show that despite the advantage of LE bumps beyond post-stall AOA, heights of the bumps have influence on performance of the airfoil as well. Among the various bumps sizes (heights) tested, bump's height of 6% chord length shows better performance. More recently, a research work that studied influence of inter-bumps distances (spacing) at airfoil LE using same cross-section profile used by Kunya *et al.,* [13] show that performance due to LE bumps depends on Reynolds number and bumps spacing only at larger AOA beyond stall angle. The study was conducted by Kunya *et al.,* [14] at Re of 2.5 X 10^4, 4.9 X 10^4, and 7.2 X 10^4. As Re increases performance increases between 0- and 15-degree AOA. Bumps spacing has effect on the airfoil performance at low air velocity (that is, low Re) at AOA in the range, 12 to 25 degrees.

LE of wind turbine rotor blade was modified and examined using 3-D computational dynamic method (CFD) by Kunya *et al.,* [15] at low Re and 6-degree AOA. The LE of the blade was modified with sinusoidal bumps, and on comparison with unmodified blade it shows that the modified blade performed better than the conventional one; according to them could be that bumps control passive flow which could as a result improve the performance of the blade. Similarly on three-dimensional study, Bellequant and Laurence [16] reported the performance examination results of the 5-metre (prototype) whale power wind turbine blades (incorporating tubercles along its LE. The measurement was conducted by the Canada Institute of wind energy, North Cape, Prince Edward Island. Measurements were taken using a Wenvor 25 kW wind turbine on which the blades were installed. The whale power (modified) blades have a greater power curve slope and reached rated power at around 12.5 m/s whereas the Wenvor blades reached rated power at around 15 m/s. For the modified wind turbine blades, the peak coefficient of power (Cp) attained is around 0.4.

There are many research works on performance of airfoil reviewed ([17-19] to mention some) but did not consider LE bumps modification. The review of the past works on LE bumps influence on airfoil performance brought the knowledge that bumps could improve the working angle of airfoil beyond stall angle of a normal unmodified airfoil LE, providing greater aerodynamic boost, and gentle stall trend. Size of bump, type of airfoil profile, and Reynold number are the important performance dependent variables on which LE bumps modification might depend. However, from obtainable

works, no research work done on modification of rotor blade (which has NASA LS (1)-0413 profile) of micro wind turbines with LE bumps, and by varying tip speed ratio (TSR) and Re. around 10^4.

2. Methodology

In this work CFD tools were used for the numerical analysis of wind turbine blades (WTB) performance due to the effect of modification at their leading edge by introducing sinusoidal bumps. Two CAD models of full span WTB were developed based on 0.8m three-bladed wind turbine rotor. One model is having straight leading edge (Normal Blade or N-Blade) whereas the other having LE bumps (Modified Blade or M-Blade; bumps height = 6% chord length; bumps spacing = 40% blade span). Both models have NASA LS (1)-0413 cross-section profile. The LS (1) represent low speed first series, the first two digits after the dash represent the design lift coefficient (0.4) and the last two digits represent the maximum thickness to chord ratio (13%). Table 1 shows the co-ordinates of the NASA LS (1)-0413 airfoil section in percent of chord length (c).

Table 1
The Co-ordinates of the NASA LS (1)-0413 Airfoil Section

Station (x/c)	Upper surface Ordinate (y/c)	Lower Surface Ordinate (y/c)
0.0	0.0	0.0
0.0020	0.01035	- 0.00495
0.0050	0.01588	- 0.00935
0.0125	0.02424	- 0.01448
0.0250	0.03325	- 0.01907
0.0375	0.03966	- 0.02226
0.0500	0.04476	- 0.02498
0.0750	0.05261	- 0.02938
0.1000	0.05862	- 0.03281
0.1250	0.06347	- 0.03562
0.1500	0.06755	- 0.03792
0.1750	0.07103	- 0.03982
0.2000	0.07399	- 0.04139
0.2500	0.07861	- 0.04368
0.3000	0.08182	- 0.04484
0.3500	0.08381	- 0.04516
0.4000	0.08464	- 0.04474
0.4500	0.08435	- 0.04353
0.5000	0.08293	- 0.04144
0.5500	0.08023	- 0.03810
0.5750	0.07834	- 0.03589
0.6000	0.07605	- 0.03334
0.6250	0.07335	- 0.03051
0.6500	0.07024	- 0.02745
0.6750	0.06674	- 0.02425
0.7000	0.06287	- 0.02097
0.7250	0.05868	- 0.01767
0.7500	0.05419	- 0.01441
0.7750	0.04946	- 0.01126
0.8000	0.04450	- 0.00831
0.8250	0.03933	- 0.00568
0.8500	0.03397	- 0.00347
0.8750	0.02843	- 0.00181
0.9000	0.02275	- 0.00080
0.9250	0.01692	- 0.00058
0.9500	0.01096	- 0.00135
0.9750	0.00483	- 0.00336
1.0000	- 0.00156	- 0.00714

The coordinates (in text document type format) when imported into modelling software appear as shown in Figure 2.

Fig. 2. NASA LS (1) - 0413 Airfoil Coordinate appearance in Software

Both blades were modelled using POINTWISE software and their sizes are as shown in Figure 3. A single blade is positioned inside a fluid domain one 1m away from fluid entry face and 3m before exit, and set to rotate through 120-degree; this represents just 1/3 of complete revolution. The fluid domain length is 4m and has a truncated conical shape (Figure 4).

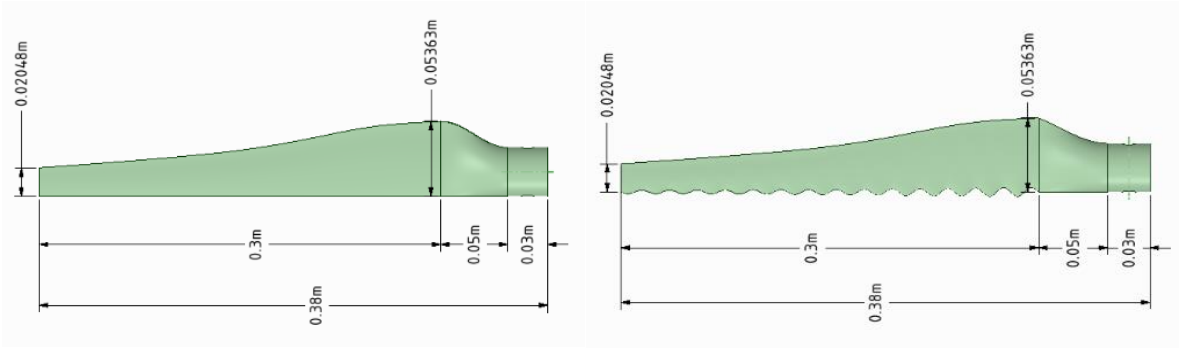

(a) (b)

Fig. 3. Diagram of the blades (a) N-Blade (b) M-Blade

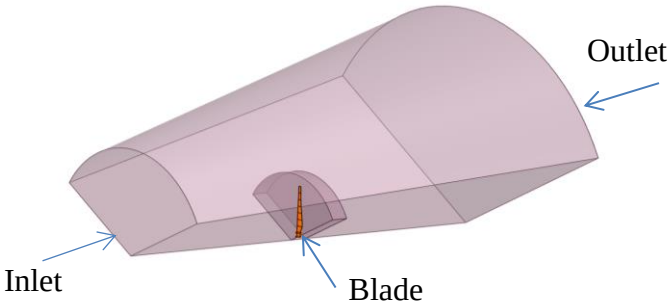

Fig. 4. Diagram of the flow domain showing the blade

Approximately 4.5 x 10^6 unstructured mesh cells were created inside the fluid domain to ensure accurate resolutions of flow variables. Figure 5 shows the fluid domain that is meshed.

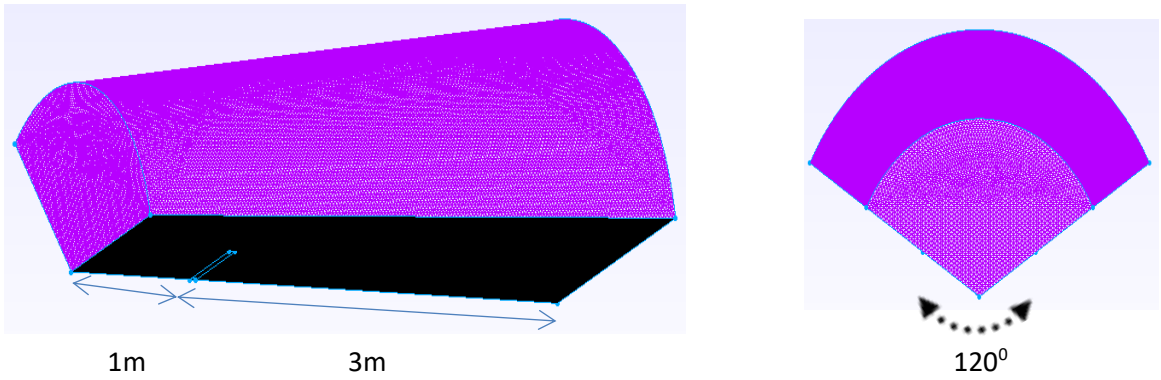

Fig. 5. Diagram showing the meshing and dimension of the flow domain

To further reduce numerical error (and correctly resolve variables) during computational in the software more cells are concentrated at and around the curve surface of LE and trailing edge (TE) of both the normal and the modified blades. See Figure 6.

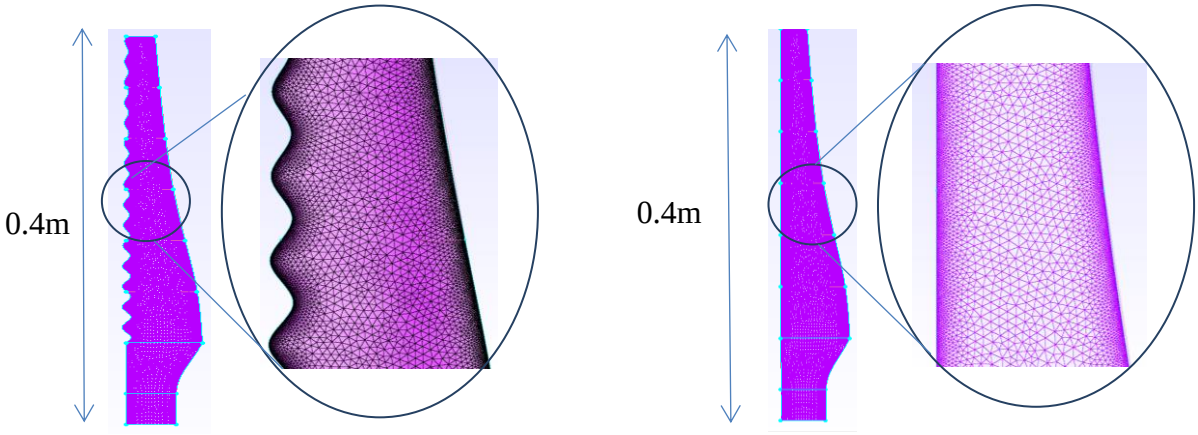

Fig. 6. Diagram showing the meshing around the blades

Simulation is carried out using the moving reference frame (MRF) method. In this method, blade remains stationary but air in the fluid domain is rotated around the blade. Blade pitch angle of 5-degree and K-Omega Standard Shear Stress Turbulent model (available in ANSYS 2020) were used in this study. A boundary layer (BL) is a thin layer of flowing fluid in contact with a surface such as WTB. A dimensionless wall distance (Y^+) magnitude determines the relative importance of viscous and turbulent processes within a BL, and it determines grid spacing in CFD. A Y^+ of below five (5) indicates a viscous or laminar region where more mesh cells are required for accurate resolution of BL. A Y^+ value of one (1) (less than the upper limit of laminar flow, which is 5) was used in this work. This resulted in generating more layers of mesh cells within the viscous region. Pseudo transient algorithm were selected from the solver numerical settings. The software was run starting with a velocity of 2 m/s to 10 m/s at the interval of 2m/s. This is done for a tip speed ratio (TSR) of 6 and 8. Simulations were further run at constant angular speed of 120 rad/s at a TSR of 2, 4, and 10.

2.1 Governing Fluid Dynamic Equations

Continuity, Navier-Stokes, and energy equations are the general equations in fluid dynamics and were derived respectively based on basic principles of mass, momentum, and energy balance [20].

$$\frac{\partial \rho}{\partial t} + \nabla.(\rho V) = 0 \quad (1)$$

(Continuity equation)

$$\rho \frac{\partial V}{\partial t} + V.\nabla(\rho V) = \nabla.\tau_{ij} - \nabla P + \rho F \quad (2)$$

(Navier-Stokes's equation)

$$\rho \frac{De}{Dt} + P(\nabla.V) = \frac{\partial Q}{\partial t} - \nabla.q + \Phi \quad (3)$$

(Energy equation)

where

$$\nabla\, is\, \left(\frac{\partial}{\partial x} + \frac{\partial}{\partial y} + \frac{\partial}{\partial z}\right)$$

The solution algorithm and numerical procedure for any kind of fluid dynamics system problem determines the number of equations and combination of their terms needs to be deployed. Depending on the nature of physics governing the fluid motion, more complex system will require more equations and their terms.

2.2 Grid Independent Study

The grid generated within the fluid domain might not resolve the fluid domain correctly, and it thus become very useful to vary the size and number of grid cells and observe how it influence the result of the simulation. Result could change significantly with varying grid resolution using same meshing scheme but when things are okay further increasing the resolution will only change the result may be insignificantly. Grid study was conducted in this work using the conventional blade (N-Blade) at 6m/s air velocity of 6m/s, 5-degree pitch angle and TSR of six (6). Table 2 shows the grid independent study results.

Table 2
Grid independent study

Grid No.	Resolution (million cells)	Torque (Nm) x 10^{-2}
1	2.27	3.55
2	3.81	4.98
3	4.53	5.50
4	4.96	5.54

The result is also represented as graph (Figure 7) for clear understanding of how grid resolution can influence solution accuracy. The torque value by using grid 1 resolution has increase significantly on improving the resolution to grid 2. The change in torque value by increasing the cell number from grid 2 to grid 3 is relatively smaller. Even though there is significant difference in terms of cells count (about 4.29 x 10^5 cells) between grid 3 and grid 4, the change in torque value is insignificant. It will

be without doubt that utilizing grid 3 rather than grid 4 can save simulation time and still preserve accuracy. Grid 3 has cells count of 4.53 million cells and it was used in this work.

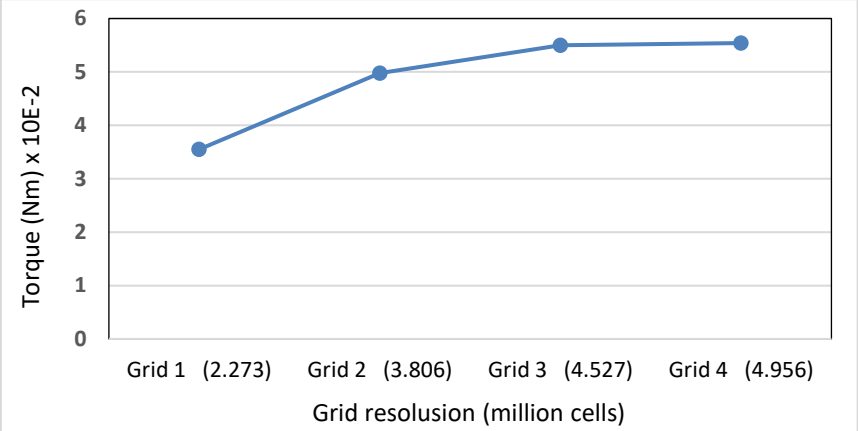

Fig. 7. Grid independent study

2.3 Boundary Conditions

The form of the boundary conditions that is required by any partial differential equation depends on the equation itself and the way that it has been discretized. The governing equation of fluid motion may result in a solution when the boundary conditions and the initial conditions are specified. This work boundary condition is that the velocity of the free air stream (V_0) is specified as inlet and outlet fluid velocities. The software solved the fluid flow equations within the fluid domain for pressure and velocity fields, and then other performance parameters were calculated

2.4 Aerodynamic Forces and Equations used for Blade Design and Results Analysis

A fluid diverts from its original path when flowing past an airfoil which and causes variation in the fluid pressure and velocity. Friction or drag force affect the fluid flow because of its viscosity. The drag force and the lift force are together the effective force applied by the fluid on the airfoil or any other solid body, it is called the aerodynamic force. The direction of the aerodynamic forces applied by fluid on solid surface of airfoil is shown in Figure 8.

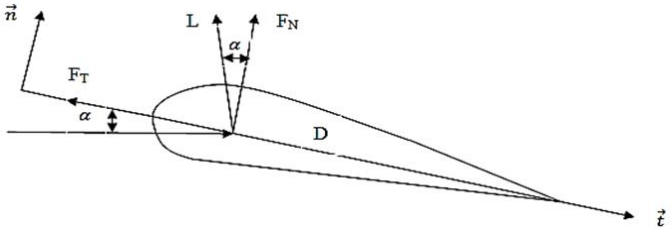

Fig. 8. Airfoil Aerodynamic forces

Eq. (4) to Eq. (9) provide Mathematical relations (4-9) were used for sizing the blades and examination of results. Optimal chord length (C_{opt}) across the entire length of the blade were determined using [21]

$$C_{opt} = \frac{2\pi r}{B}\frac{8}{9C_L}\frac{V}{\lambda V_r} \tag{4}$$

The formula for determination of blade pitch angle (β) at a radial station (r) is given by Schubel and Crossley [21] as

$$\beta(r) = tan^{-1}\left(\frac{2R}{3r\lambda}\right) - \alpha \quad (5)$$

Tip speed ratio (λ) and angular velocity (ω) [21]

$$\lambda = \frac{V_t}{V} \quad (6)$$

$$\omega = \frac{V}{r} \quad (7)$$

Relations for determining rotor power (P) and performance coefficient are (C_P) [22]

$$P = T\omega \quad (8)$$

$$C_p = \frac{P}{\frac{1}{2}\rho AV^3} \quad (9)$$

2.5 Data Validation

Betz limit (0.593) is the extreme theoretical amount of performance coefficient of wind turbine [22]. The average value of C_p of the N-Blade and M-Blade's rotors (0.29025) simulated at 6m/s wind speed in this work did not reach this limit. The main reason why the C_p value did not reach Betz limit is that the size of the wind turbine is very small and the rotor blades have no twist; this is part of this work limitations that M-Blade could not be twisted. A study by Hsiao *et al.,* [23] revealed that lack of blade twist could reduce C_p by significant amount. The result of this research work is thus validated.

3. Results

Simulations in this work were run from a velocity of 2 m/s to 10 m/s at the interval of 2m/s. This is done using a TSR of 6 and 8. Usually TSR of horizontal axis wind turbine (HAWT) is between 6 and 8. Also in this study simulations were further run at constant angular velocity of 120 rad/s for a TSR of 2, 4, and 10. Single blade is considered during the process and extrapolated the result for 3 blades. The torque values attained and by using Equations 8 & 9, the C_P values of the rotor blades were determined. The C_P values are then multiplied by 3 to account for 3 blades; the plots are based on the C_P values of 3-bladed turbine rotor.

3.1 Power Coefficient Versus Velocity at a Tip Speed Ratio (TSR) of Six (6)

Figure 9 shows the variation of power coefficient, C_P with air velocity (varied from 2m/s to 10 m/s at the interval of 2m/s) for the two models at TSR of 6. The results have shown that the C_P values from the results are not equal, with the straight blade (N-blade) having better performance than the bumpy blade (M-blade) at all velocities tested. The Cp values of blade with straight leading edge are 0.180, 0.267, 0.300, 0.313, and 0.322 while that of blade with bumpy leading edge are 0.165, 0.250, 0.281, 0.294, and 0.303 at respective velocities of 2, 4, 6, 8, and 10m/s for both blades.

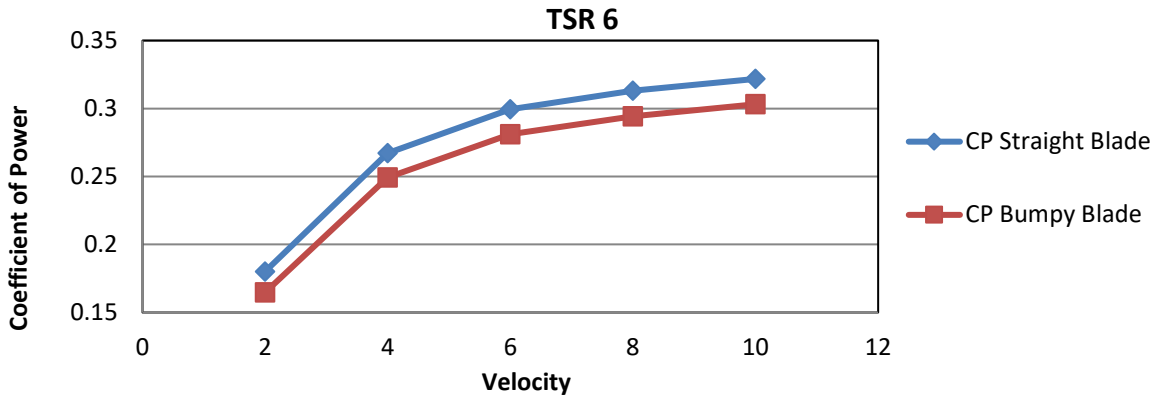

Fig. 9. Power coefficient versus. velocity at a TSR of 6

The difference in performance between the two blades is thus more obvious at a TSR of 6. The flow velocity contour plots at the surface of the two blades at different heights from the blade root to the tip at wind velocity of 8 m/s are provided and shown in Figure 10. to the show the reason why there is difference in their performances. The maximum flow velocity occurs at the blades' tips, and it can be seen in the plots that the tip speed velocity of N-Blade (46m/s) is greater than that of M-Blade (42m/s).

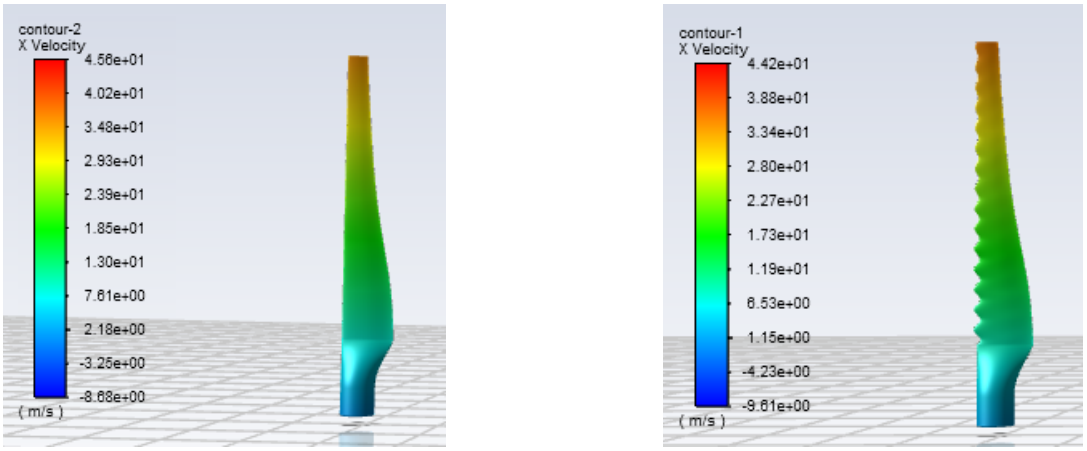

(a) (b)

Fig. 10. Flow velocity contour at the surface of the blades (a) N-Blade (b) M-Blade

3.2 Power Coefficient Versus Velocity at a TSR of Eight (8)

At a TSR of 8, the C_P values closely match for both N-Blade and M-Blade at all velocities tested as shown in Figure 11. It shows that there is insignificant or no difference in the C_P values for all the velocities.

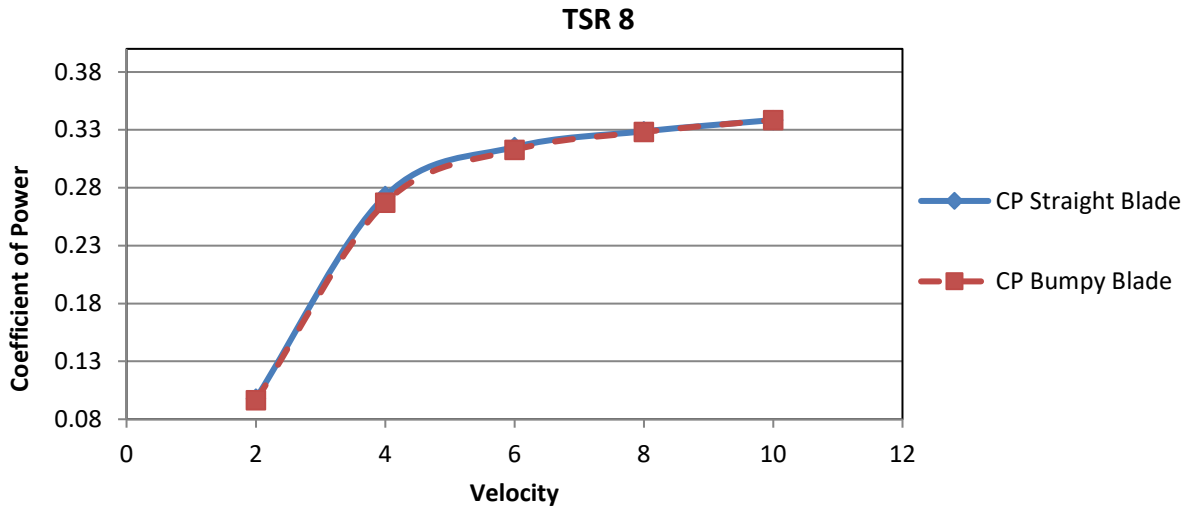

Fig. 11. Power coefficient versus velocity at a TSR of 8

3.3 Performance Curve at Constant Rotational Speed

Figure 12 shows the power coefficient versus velocity values at a constant angular velocity of 120 radians per second. This was done to develop the performance profile for the blades at a constant rotational speed.

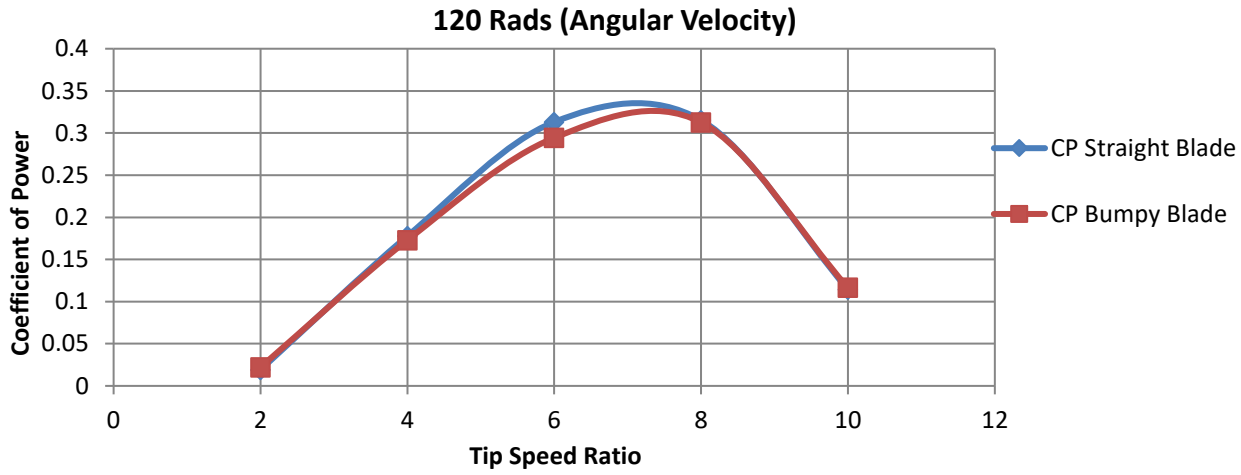

Fig. 12. Performance curves at a rotational speed of 120 radians per second

It can see from the figure that the region where the peak performance occurs is around TSR of 6 and 8. At TSR of 2, 4, 8, and 10, the performance of both airfoils closely matches except at a TSR of 6 where the N-Blade is better; the N-Blade Cp value is 0.313 and is better than that of M-Blade Cp value (0.294).

4. Conclusions

The Numerical study of wind turbine blades (WTB) performance due to the effect of modification at their leading edge by introducing sinusoidal bumps was performed using two CAD models of WTB based on 0.8m three-bladed wind turbine rotor. One blade model is having straight leading edge (N-

Blade) and the other having bumpy leading edge (M-Blade). Both models have NASA LS (1)-0413 cross-section profile. Simulations were run from a velocity of 2 m/s to 10 m/s at the interval of 2m/s considering TSR of 6 and 8. Simulations were further run at constant angular velocity of 120 rad/s for a TSR of 2, 4, and 10

i. At a TSR of 6, the C_P values are not equal, with the straight blade having better performance than the bumpy blade at all velocities tested; the Cp values of N-Blade are 0.180, 0.267, 0.300, 0.313, 0.322 at respective velocities of 2, 4, 6, 8, and 10m/s, while the Cp values of M-Blade at the same velocities are 0.165, 0.250, 0.281, 0.294, and 0.303 respectively.
ii. At a TSR of 8, the C_P values closely match for both straight and bumpy leading-edge blades at all velocities tested for.
iii. At constant angular velocity of 120 rad/s for a TSR of 2, 4, 6, 8 and 10, the peak performance occurs between TSR of 6 and 8. For instance, the Cp values of M-Blade are 0.022, 0.173, 0.294, 0.313, and 0.116 respectively at TSR of 2, 4, 6, 8, and 10.
iv. At TSR of 2, 4, 8 and 10, the performance of both airfoils closely matches except at a TSR of 6 where there is relatively significant difference; the N-Blade Cp value is 0.313 and is better than that of M-Blade Cp value (0.294).
v. It could be said conclusively that the blade leading edge modification could not have advantage at all flow conditions and size of the HAWT blades; it shows no advantage on the performance of the rotor blade tested in this research at the velocities at which the simulation was conducted.

Conflict of Interest Statement

The authors declare that there is no conflict of interest.

Acknowledgement

The authors acknowledge the full financial support received from Tertiary Education Trust Fund (TETFund) in Nigeria, under Institutional Based Research (IBR) Programme funds for Kano University of Science and Technology, Wudil researchers, TETFUND/DESS/UNI/WUDIL/RP/2018/VOL.1.

References

[1] Pam, G. Y. "Potential of Wind Energy Utilisation in Northern States of Nigeria." *PhD diss., Ph. D Dissertation, Ahmadu Bello University, Zaria, Nigeria* (2008).
[2] Ahmed, Abdullahi, A. Ademola Bello, and Dandakuta Habou. "An evaluation of wind energy potential in the northern and southern regions of Nigeria on the basis of Weibull and Rayleigh models." *American Journal of Energy Engineering* 1, no. 3 (2013): 37-42. https://doi.org/10.11648/j.ajee.20130103.11
[3] Oyewole, J. A., and T. O. Aro. "Wind speed pattern in Nigeria (a case study of some coastal and inland areas)." *Journal of Applied Sciences and Environmental Management* 22, no. 1 (2018): 119-123. https://doi.org/10.4314/jasem.v22i1.22
[4] Fish, Franke E., and Juliann M. Battle. "Hydrodynamic design of the humpback whale flipper." *Journal of morphology* 225, no. 1 (1995): 51-60. https://doi.org/10.1002/jmor.1052250105
[5] Miklosovic, D. S., M. M. Murray, L. E. Howle, and F. E. Fish. "Leading-edge tubercles delay stall on humpback whale (Megaptera novaeangliae) flippers." *Physics of fluids* 16, no. 5 (2004): L39-L42. https://doi.org/10.1063/1.1688341
[6] Clapham, Phillip J. "Humpback whale: Megaptera novaeangliae." In *Encyclopedia of marine mammals*, (2018): 489-492. https://doi.org/10.1016/B978-0-12-804327-1.00154-0
[7] Hansen, Kristy L., Richard M. Kelso, and Bassam B. Dally. "Performance variations of leading-edge tubercles for distinct airfoil profiles." *AIAA journal* 49, no. 1 (2011): 185-194. https://doi.org/10.2514/1.J050631
[8] Gawad, Ahmed Farouk Abdel. "Numerical simulation of the effect of leading-edge tubercles on the flow characteristics around an airfoil." In *International Mechnaical Engineering Congresss & Exposition*. 2012.

[9] Čarija, Zoran, Emil Marušić, Zdenko Novak, and Sanjin Fućak. "Numerical analysis of aerodynamic characteristics of a bumped leading edge turbine blade." *Engineering Review: Međunarodni časopis namijenjen publiciranju originalnih istraživanja s aspekta analize konstrukcija, materijala i novih tehnologija u području strojarstva, brodogradnje, temeljnih tehničkih znanosti, elektrotehnike, računarstva i građevinarstva* 34, no. 2 (2014): 93-101.
[10] Asli, Majid, Behnam Mashhadi Gholamali, and Abolghasem Mesgarpour Tousi. "Numerical analysis of wind turbine airfoil aerodynamic performance with leading edge bump." *Mathematical Problems in Engineering* 2015 (2015). https://doi.org/10.1155/2015/493253
[11] Zhao, Ming, Mingming Zhang, and Jianzhong Xu. "Numerical simulation of flow characteristics behind the aerodynamic performances on an airfoil with leading edge protuberances." *Engineering Applications of Computational Fluid Mechanics* 11, no. 1 (2017): 193-209. https://doi.org/10.1080/19942060.2016.1277165
[12] Munshi, Adnan, Erwin Sulaeman, Norfazzila Omar, and Mohammad Yeakub Ali. "CFD analysis on the effect of winglet cant angle on aerodynamics of ONERA M6 wing." *Journal of Advanced Research in Fluid Mechanics and Thermal Sciences* 45, no. 1 (2018): 44-54.
[13] Kunya, Bashir Isyaku, Clement O. Folayan, Gyang Yakubu Pam, Fatai Olukayode Anafi, and Nura Muaz Muhammad. "Experimental and Numerical Study of the Effect of Varying Sinusoidal Bumps Height at the Leading Edge of the NASA LS (1)-0413 Airfoil at Low Reynolds Number." *CFD Letters* 11, no. 3 (2019): 129-144.
[14] Kunya, Bashir Isyaku, Clement O. Folayan, Gyang Yakubu Pam. "A Numerical Study on the Effect of Bumps Spacing at the Leading Edge of Whale inspired NASA LS (1)-0413 Aerofoil at Low Wind Speed." *Bayero Journal of Engineering and Technology (BJET)*16, no.1 (2021): 119-132.
[15] Kunya, Bashir Isyaku, Clement Olaloye Folayan, Gyang Yakubu Pam, Fatai Olukayode Anafi, and Nura Mu'az Muhammad. "Performance study of Whale-Inspired Wind Turbine Blade at Low Wind Speed Using Numerical Method." *CFD Letters* 11, no. 7 (2019): 11-25.
[16] Howle, Laurens E. "Whalepower Wenvor Blade: A report on the efficiency of a whalepower corp. 5 meter prototype wind turbine blade." (2009).
[17] Ali, Jaffar Syed Mohamed, and M. Mubin Saleh. "Experimental and numerical study on the aerodynamics and stability characteristics of a canard aircraft." *Journal of Advanced Research in Fluid Mechanics and Thermal Sciences* 53, no. 2 (2019): 165-174.
[18] Hakim, Muhammad Syahmi Abdul, Mastura Ab Wahid, Norazila Othman, Shabudin Mat, Shuhaimi Mansor, Md Nizam Dahalan, and Wan Khairuddin Wan Ali. "The effects of Reynolds number on flow separation of Naca Aerofoil." *Journal of Advanced Research in Fluid Mechanics and Thermal Sciences* 47, no. 1 (2018): 56-68.
[19] Tajuddin, Nurulhuda, Shabudin Mat, Mazuriah Said, and Shumaimi Mansor. "Flow characteristic of blunt-edged delta wing at high angle of attack." *Journal of Advanced Research in Fluid Mechanics and Thermal Sciences* 39, no. 1 (2017): 17-25.
[20] Ashgriz, Nasser, and Javad Mostaghimi. "An introduction to computational fluid dynamics." *Fluid flow handbook* 1 (2002): 1-49.
[21] Crossley, Richard J. "Wind turbine blade design." In *Wind Turbine Technology*, pp. 23-56. Apple Academic Press, 2014. https://doi.org/10.3390/en5093425
[22] S. Rao and B. Parulekar, "Energy Technology," *Khanna publishers*, (2005).
[23] Hsiao, Fei-Bin, Chi-Jeng Bai, and Wen-Tong Chong. "The performance test of three different horizontal axis wind turbine (HAWT) blade shapes using experimental and numerical methods." *Energies* 6, no. 6 (2013): 2784-2803. https://doi.org/10.3390/en6062784